

# Structure of a complex carbonate aquifer by magnetic, gravity and TDEM prospecting in the Jaén area, Southern Spain

A. RUIZ-CONSTÁN<sup>1</sup> A. PEDRERA<sup>2</sup> S. MARTOS-ROSILLO<sup>1</sup> J. GALINDO-ZALDÍVAR<sup>2,3</sup>  
C. MARTÍN-MONTAÑÉS<sup>1</sup> J.P. GONZÁLEZ DE AGUILAR<sup>1</sup>

<sup>1</sup> Instituto Geológico y Minero de España (IGME)

Urb. Alcázar del Genil 4, Edificio Zulema, 18006 Granada, Spain. Ruiz-Constán E-mail: a.ruiz@igme.es

<sup>2</sup> Instituto Andaluz de Ciencias de la Tierra (CSIC)

Avda. de Las Palmeras 4, 18100 Granada, Spain

<sup>3</sup> Departamento de Geodinámica, Universidad de Granada

Campus Fuentenueva s/n, 18071 Granada, Spain

## ABSTRACT

Knowledge of aquifer geometry is essential for efficient and sustainable groundwater management, particularly in carbonate aquifers due to uncertainties inherent to karstic systems. The geological structure and hydrogeological continuity of Los Chotos-Sazadilla-Los Nacimientos and La Serreta-Gante-Cabeza Montosa carbonate aquifers (Jaén; SE Spain) have been established through structural measurements, geophysical prospecting –magnetic, gravity and time-domain electromagnetics (TDEM)– and the study of piezometric levels. Yet the scarce hydrogeological data, the complexity of the tectonic structure and the presence of Plio-Quaternary rocks covering the highly permeable carbonate rocks make it difficult to establish a robust conceptual hydrogeological model of the aquifer. This study focuses on an area where hydrogeological disconnection between the two aquifers was traditionally assumed, given the diapiric emplacement of low permeable rocks between them. The new geophysical data demonstrate connection between aquifers that implies greater groundwater reserves than previously supposed. This field example supports the suitability of the combined use of electromagnetic methods with gravity and magnetic research that have been poorly combined up to recent times for hydrogeological studies.

**KEYWORDS** Carbonate aquifer. Potential field research. Electromagnetic prospecting. Betic Cordillera. Groundwater resources. Hydrogeological continuity.

## INTRODUCTION

The structural knowledge of geologically complex aquifers not belonging to the main sedimentary basins (18% of the earth surface; WHYMAP, 2008) is of great relevance, as they represent the main water supply in many arid areas. This is even more important in carbonate aquifers, given the uncertainties inherent to karstic systems (Bakalowicz, 2005). Quantification of groundwater resources thus becomes a top priority

when designing efficient and sustainable management policies, and research must be focused on the definition of hydraulic parameters, the vertical/lateral limits of the outcropping carbonate system, and the contact with other non-permeable formations (Foster *et al.*, 2006). A multi-method approach –integrating information from geology, hydrology, and diverse geophysical techniques– implies significant reduction in uncertainty (Tronicke and Holliger, 2005; Soupios *et al.*, 2007; Duque *et al.*, 2008; Dafflon *et al.*, 2009), allowing the storage, flow path and evolution

of a groundwater system to be constrained and quantified (Chalikakis *et al.*, 2011).

Today, electrical and electromagnetic methods – including time-domain electromagnetics (TDEM)– are successfully and widely applied for subsurface imaging, as they allow for relatively fast and detailed mapping (Chambers *et al.*, 2006; Nielsen *et al.*, 2007; Martos-Rosillo *et al.*, 2014). Inversion of this kind of data produces non-unique models, while its combination with other information constrains the number of solutions and enhances interpretation. In addition, gravity data are essential to study the variation in sedimentary thickness of basins (Kamer *et al.*, 2005; Ruiz-Constán *et al.*, 2009) or to check the suitability of proposed complex cross sections (Ayarza *et al.*, 2005; Ruiz-Constán *et al.*, 2012).

Although the use of magnetic techniques in regional surveys, the hydrocarbon industry or mineral prospecting started at the beginning of the twentieth century (Smyth, 1896; Wantland, 1944; Peters, 1949), little use has been made strictly for groundwater research. In recent years, magnetic data acquisition using airborne measurement systems has become generalized in the study of basins due to the improvement and cheapening on their application, providing valuable information on basements in vast areas (Finn and Morgan, 2002; Mishra and Vijay Kumar, 2005). Yet when dealing with small aquifers having a complex geological structure, where the magnetic anomalous bodies are scarce and anomalies have a smaller wavelength, magnetic data acquisition does not provide enough resolution, and ground-based acquisition emerges as necessary (Gibson *et al.*, 1996; La Femina *et al.*, 2002).

Water supply in SE Spain (dry Mediterranean climate) is mainly derived from groundwater resources (85%; IGME-DPJ, 2011) and aquifers were declared overexploited up to 2027 by the Spanish Government in view of their declining levels and high exploitation rate (166%). In this study, we jointly analyse magnetic and gravity data in addition to TDEM soundings to characterize the deep geological structure of a carbonate aquifer with structural complexity: the Los Chotos-Sazadilla-Los Nacimientos (LSL) aquifer. Geophysical prospecting is integrated here with geologic and hydrogeologic data in order to redefine the hydrogeological continuity between the different carbonate outcrops and with an adjacent aquifer known as La Serreta-Gante-Cabeza Montosa (LGC).

## GEOLOGICAL AND HYDROGEOLOGICAL SETTING

The LSL aquifer is located in Jaén (SE Spain) and constituted by rocks belonging to the External Zones of the Betic Cordillera, the westernmost part of the Alpine

Mediterranean Belt (Fig. 1). They are mainly formed by carbonate and detritic sedimentary rocks that also include volcanic rocks, deposited over the southern margin of the Iberian variscan basement from the Mesozoic up to the Lower Miocene (García-Hernández *et al.*, 1980). The External Zones are affected by thin-skinned deformation since the Upper Oligocene (~25Ma) and have a fold-and-thrust belt structure (Pedrera *et al.*, 2013). On the basis of paleogeographic features they have traditionally been subdivided into the Prebetic and Subbetic, the latter cropping out widely in the study area (Ruiz Reig *et al.*, 1988a, b).

The stratigraphic sequence of this region (Fig. 2) starts with Triassic sandstones, clays and evaporites (Pérez-López, 1991, 1996) overlaid by dolomitized Lower Jurassic limestones. During a Jurassic-Cretaceous transtensive stage, basic pillow-lavas were interstratified within the Subbetic rocks. The sedimentary sequence continues with oolitic limestones, radiolaritic marls, marly limestones and nodular limestones of Late Jurassic age. The Lower Cretaceous is characterized by white marls and marly limestones, whereas the Upper Cretaceous and the Paleogene are formed by reddish marls and marly limestones. During the Eocene and up to the Tortonian, marls and calcarenites were deposited, while the Plio-Quaternary is constituted by continental lutites, sandstones and conglomerates (Vera, 2004).

The LSL aquifer comprises a series of carbonate outcrops (Ruiz Reig *et al.*, 1988a, b): 9km<sup>2</sup> of Lower Jurassic dolostones with a maximum thickness of 300m (Cerro de los Peones, Cerro Los Chotos) to the East, together with 20km<sup>2</sup> of Lower Miocene bioclastic calcarenites having a thickness up to 100–120m in the western sector (Fig. 1B). The substrate is constituted by low permeability Triassic clays and marls (Pérez-López, 1991, 1996). The renewable resources of the aquifer were estimated at 2.4hm<sup>3</sup>/year (IGME-DPJ, 2011) and their lateral limits are not fully known. Triassic rocks crop out to the N, W and S, closing these borders to groundwater flow. However, the nature of the SE border, covered by semi-permeable Plio-Quaternary rocks, remains controversial (Fig. 1).

Information about the hydraulic parameters of the aquifer is very limited. The pumping test of Cerro de los Peones (D) give an average transmissivity value of 9950m<sup>2</sup>/day and a storage coefficient of 2x10<sup>-2</sup> (ITGE, 1990). Figure 1 shows the hydrogeological information available. Los Nacimientos spring (B), the main drainage point of the western sector, is at a height of 996m.a.s.l., considerably higher than the rest of the aquifer. On the other hand, the piezometric level at Cerro de Los Peones (944m.a.s.l. in July 2013) and Molino del Barranco spring (C, 932m.a.s.l.) suggests that the eastern sector of the aquifer has the same

altitude as Molino de Gante spring (F, 939m.a.s.l. in July 2013) and its near piezometer (E). This information points to hydrogeological continuity among the Jurassic outcrops of the eastern sector, from Cerro de los Chotos up to Molino de Gante spring (F, main drainage point of LGC aquifer).

The cumulated piezometric decrease between April 2004 and August 2009 was 34 meters (Fig. 3). During the period of intensive rain since 2009, the piezometric level increased over the height of the Molino del Barranco spring (C, 932m.a.s.l.). In dry periods, the piezometric levels drop rapidly, especially when Molino del Barranco spring is active, and when extractions take place at the pumping sounding of Cerro de Los Peones (D, Fig. 1). This significantly decreasing rate could be justified by the presence of impermeable borders that accelerate the

depression level of the pumping cone around the well. However, after intensive rainfall years, the level recovery is very fast, suggesting the existence of important storage reserves.

Traditionally, Cabeza Montosa and other carbonate reliefs cropping out to the south of the LSL aquifer have been assigned to the so called La Serreta-Gante-Cabeza Montosa (LGC) aquifer. This system is composed by two antiforms and a synform of Middle-Upper Jurassic carbonate rocks with interstratified volcanic rocks (ITGE, 1990). Along its SE border there are two discharge points: the Molino de Gante spring (F) at 939m.a.s.l., with a flow in the range of 18–44l/s; and the pumping well of Molino de Gante (E). Hidden discharge towards the detritic Plio-Quaternary rocks with a moderate permeability is reported around the eastern border.

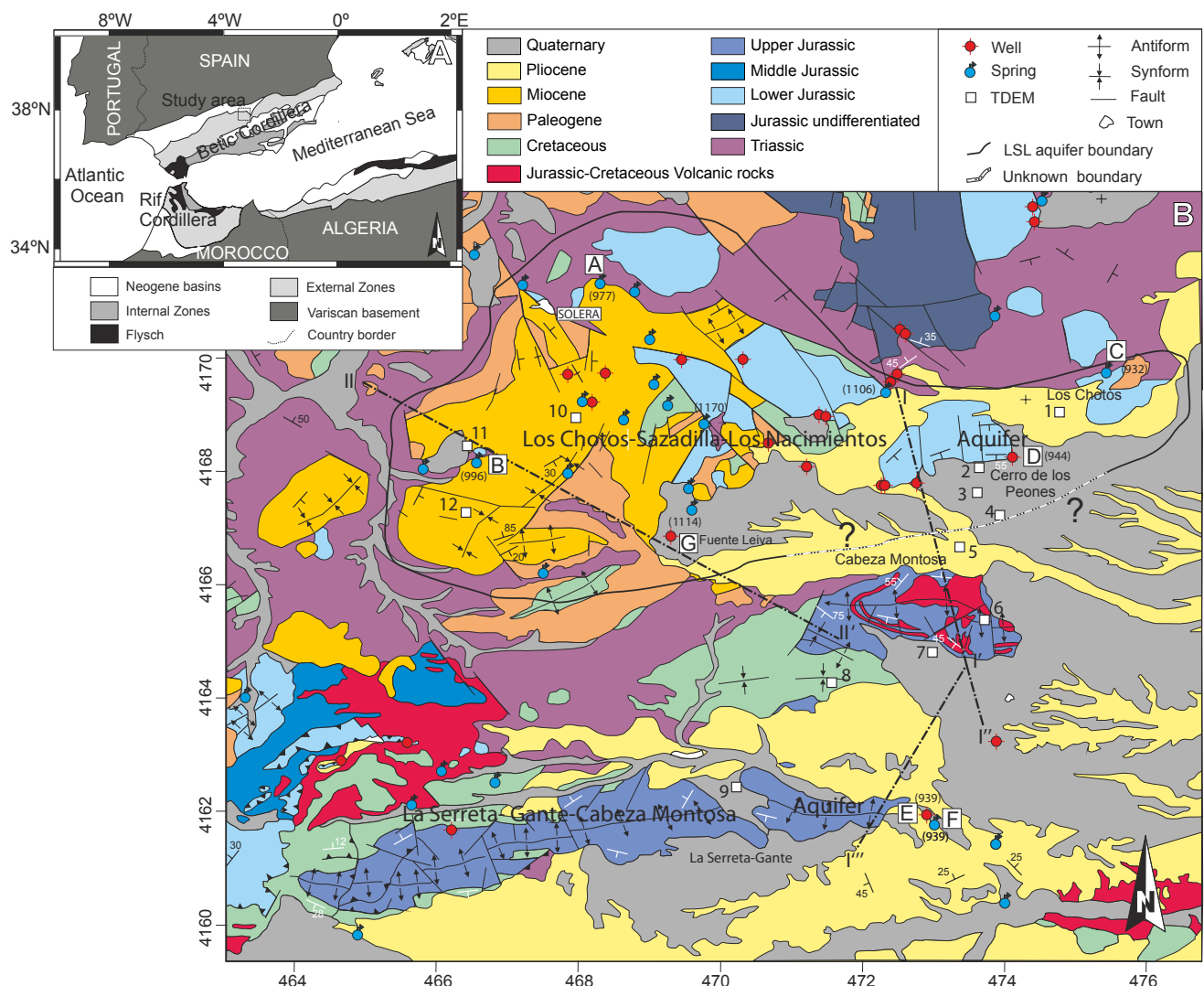


**FIGURE 1.** A) Geological map of the study area in the framework of the Betic-Rif Cordillera B) Geological map of the study area of the LSL aquifer (surrounded by a black line) and the adjacent LGC aquifer. The analysed discharge points are: Fuente de las Negras spring (A), Los Nacimientos spring (B), Molino del Barranco spring (C), Cerro de Los Peones sounding (D), Molino de Gante sounding (E), Molino de Gante spring (F), Fuente Leiva sounding (G) and El Nacimiento (H). In parentheses, the piezometric level in July 2013. Transects are marked.

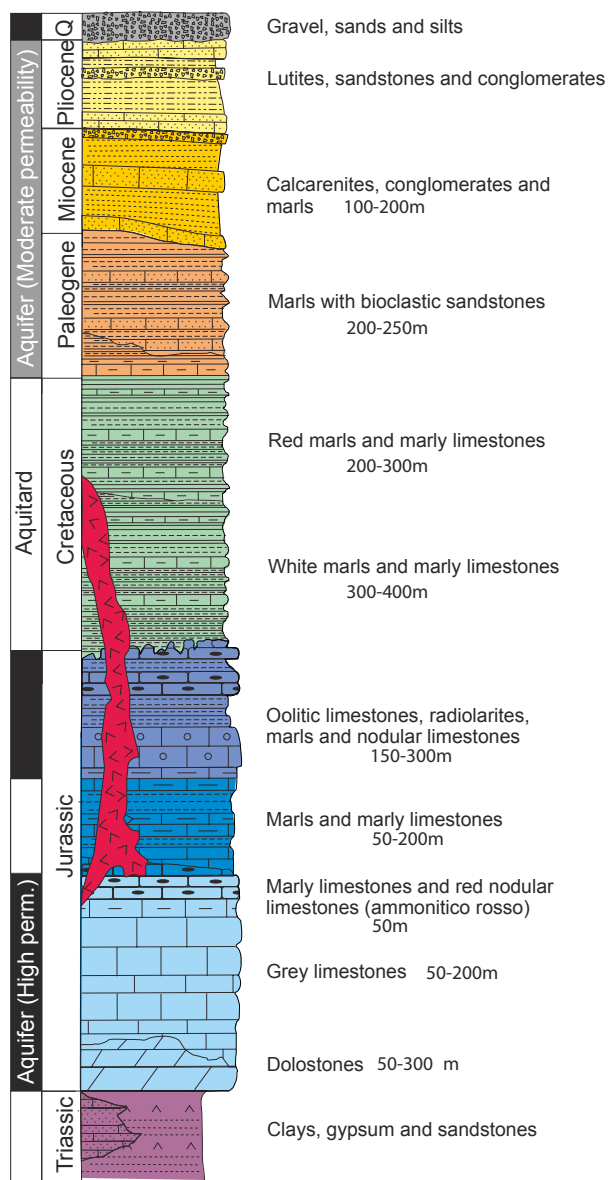


**FIGURE 2.** Lithological sequence (see Figure 1 for legend) and hydrogeological properties of the rocks (black, aquifer with high permeability; grey, aquifer with moderate permeability; white, aquitard) of the studied sector.

## METHODOLOGY

Magnetic, gravity and TDEM data were gathered in order to determine the deep geological structure and the connection of the two previously described aquifers. In addition, structural and hydrogeological data were integrated aiming to better constrain the geophysical models carried out.

### Gravity data

Gravity prospecting involves measurements of variations in the gravitational field of the earth aiming to

locate local masses of higher or lower density than the surrounding formations through the study of the observed anomalies. Gravity data were acquired using a Scintrex Autograv CG-5 gravity meter with a maximum accuracy of 0.001mGal. Data acquisition was carried out in cycles of one day as the gravity meter automatically performs the tidal correction, avoiding successive returns to the base station. Horizontal position was determined with a Garmin Dakota GPS navigator of accuracy higher than 5m. The station height was afterwards fixed using the 5m Digital Elevation Model of the Instituto Geográfico Nacional (IGN; <http://centrodedescargas.cnig.es/CentroDescargas/index.jsp>) with centimetric vertical accuracy. In addition, during the measurement cycles, a barograph located near the base station was used to correct apparent diurnal variations in elevation due to atmospheric pressure evolution.

Measurements were referenced to the Granada base station of the Instituto Geográfico Nacional's gravimetric network (<http://www.ign.es/ign/main/index.do>), to calculate the absolute gravity value. A total of 210 new field data (Fig. 4A), spaced at an average of 250–300m, were acquired along several profiles covering the whole study area. These data were integrated with 99 additional gravity measurements from the IGME database (<http://cuarzo.igme.es/sigeco/default.htm>) to better constrain the Bouguer anomaly. The terrain correction was obtained by means of Hammer circles (Hammer, 1982) for a distance of 2.6km from the stations (B-H zones), using the 5m IGN digital terrain elevation model, and up to 22km (I-M zones) applying the SRTM3 NASA digital terrain elevation model (<http://www2.jpl.nasa.gov/srtm/>) with a 90m cell size. Complete Bouguer anomaly was determined with a standard density of 2.6 g/cm<sup>3</sup>, typical of the sedimentary rocks of the External Zones of the Betic Cordillera, and considering the GRS67 Geodetic Reference System.

The 2D gravity models (Fig. 5) were calculated using GRAVMAG V.1.7 software of the British Geological Survey (Pedley *et al.*, 1993). This software makes it possible to remove the regional trend, depending on the regional geological structure, and isolate the residual anomaly associated with the rocks forming the aquifer and its basement. However, there is not an unique solution to explain an observed anomaly, and other data (*i.e.* magnetics) are necessary to further constrain the models.

### Magnetic data

Simultaneous to gravity data acquisition, 209 total magnetic field measurements (Fig. 4B) were gathered using a GSM 8 proton precession magnetometer with an accuracy of 1nT. Measurements were done at a mean height of 2m above the topography. Susceptibility of the pillow lavas was measured by means of an Exploranium KT-9 kappameter,

which averages 10 measurements at each available outcrop. Mean spacing along successive measurements was 250x300m. Electric power lines or ferromagnetic material distort the natural magnetic field, so magnetic measurements were not acquired near anthropic settlements.

Total field magnetic anomalies were calculated through a standard procedure including reduction to the IGRF 2010 (IAGA working group V-MOD, 2010). Diurnal variations were corrected using the continuous recording of the nearest Intermagnet observatory ([www.intermagnet.org](http://www.intermagnet.org)), located at the Real Observatorio de la Armada in San Fernando (Cádiz). Measurements were gathered daily in the same time period, and the magnetic observatory generally revealed low variability of the magnetic field during acquisition periods. The 2D magnetic models (Fig. 5) were calculated using GRAVMAG V.1.7 software (Pedley *et al.*, 1993) which allows modelling the residual magnetic anomaly by removal of the regional trend from the total field magnetic anomaly.

### TDEM soundings

TDEM is an electromagnetic induction method where the earth is energized with a loop of current on the surface (Kirsch, 2009). The exciting current is turned off at different time delays and the vertical component of the resultant magnetic field is measured after the primary fields disappear. The amplitude and rate of decay of these secondary fields are measured at the surface and analysed in terms of the variation of electrical resistivity with depth.

Twelve TDEM soundings were performed within the two areas of interest (Figs. 1 and 6). Data were acquired

with a ZONGE Engineering's system constituted by a 16-channel GDP32II receiver, a ZT-30 transmitter and a TEM-3 antenna. Three different frequencies (4, 8 and 16Hz) were measured using 200x200m loops in areas with low electromagnetic noise and smooth topography that provide good quality data and survey depths of up to 400–600m. Voltage/time transients were transformed to resistivity/time and inverted through smooth-model inversion into one-dimensional layered models with the industry-standard STEMINV program. Layer thicknesses are fixed by calculating source-field penetration depths for each window time. Layer resistivities are then adjusted iteratively until the model TEM response is as close as possible to observed data, consistent with smoothness constraints (Figs. 6 and 7). Smooth-model inversion does not require any a priori estimates of model parameters and the result is a set of estimated resistivities which vary smoothly with depth.

## RESULTS

Magnetic, gravity and TDEM data are combined to characterize the variations of the physical parameters of underground formations. As their inversion produce non-unique models, the comparison of results from each geophysical method allows us to better constrain the complex tectonic structure of the carbonate aquifer and its compartmentalization.

### Gravity models

The Bouguer anomaly shows a southwards decreasing trend related to the continental crust thickening, with an

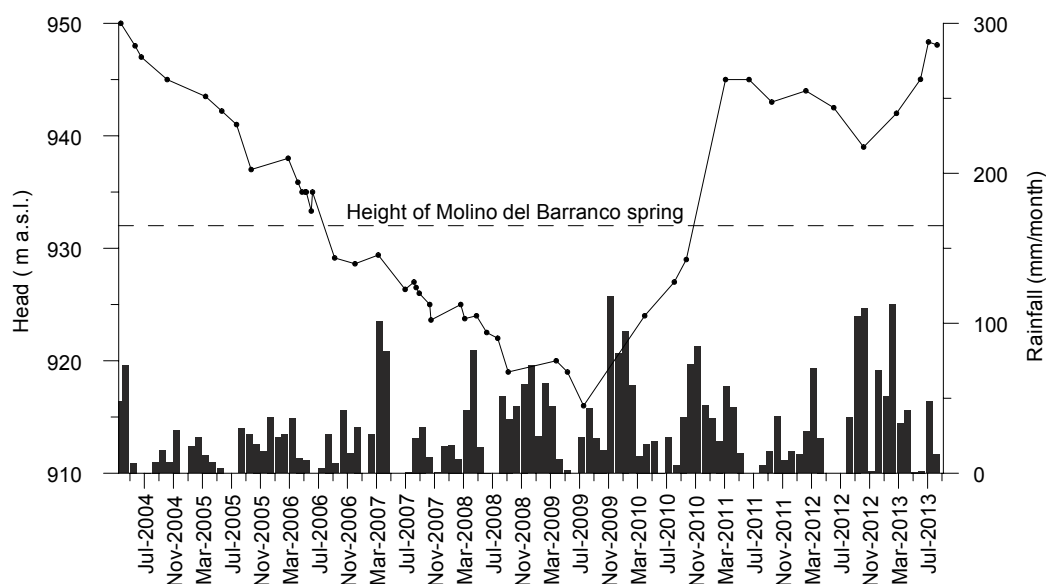
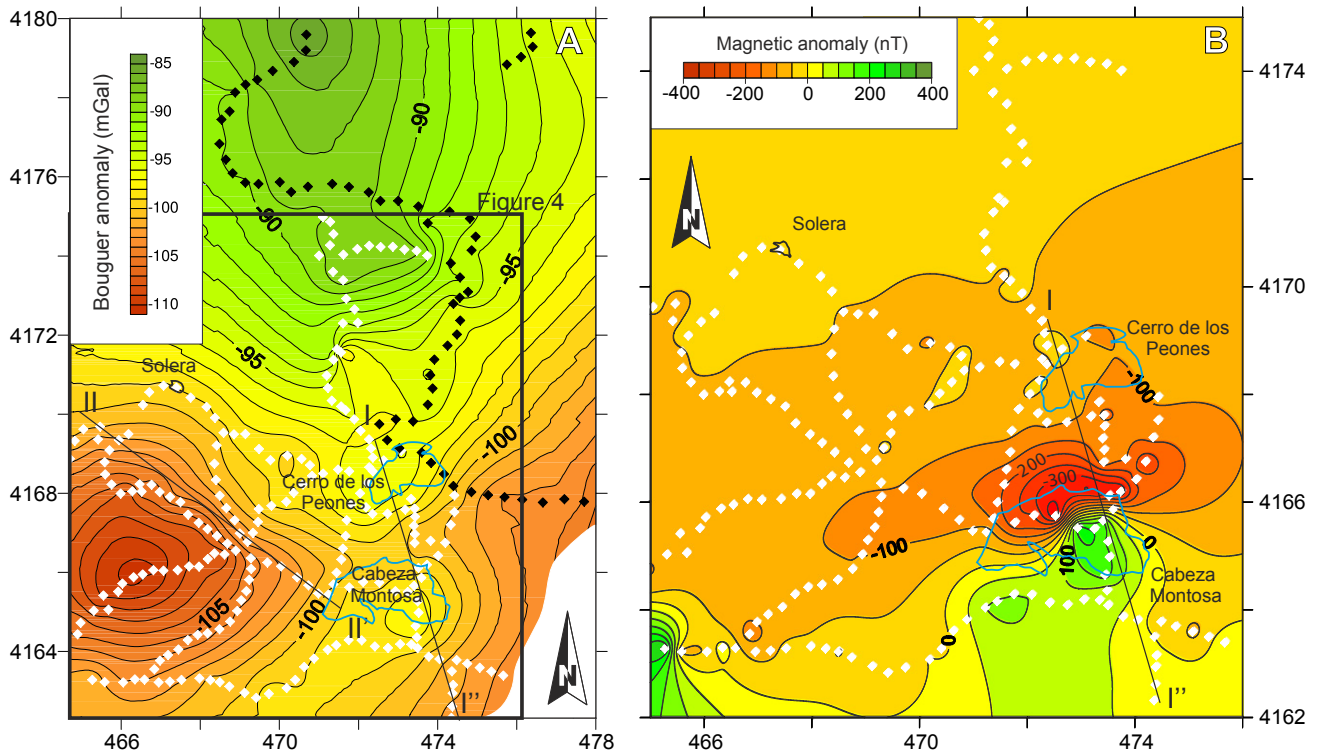


FIGURE 3. Piezometric evolution of Cerro de Los Peones pumping sounding (D in Fig.1).





**FIGURE 4.** A) Bouguer anomaly map and B) Total Field magnetic anomaly map. White symbols are data acquired in this study; black symbols correspond to the IGME database. The profiles modeled are marked. Blue contours correspond to the main carbonate outcrops of Cabeza Montosa and Cerro de Los Peones, the village of Solera is represented by a black polygon.

average gradient of 2mGal/km (Fig. 4A). The gravity maximum is located at the N edge of the study area (-85mGal), while the minimum (-111mGal) has an equidimensional shape and is found 5km south of Solera, in a region with wide outcrops of Neogene and Triassic rocks. Bouguer anomaly values at the main hills of Cabeza Montosa and Cerro de los Peones are -95mGal and -97mGal, respectively. Between them, there is another relative minimum of -100mGal.

Two 2D gravity models have been performed (Fig. 4A). The I-I' profile, crossing Cerro de los Peones and Cabeza Montosa, and the II-II' profile with a N130° direction and crossing the negative Bouguer anomaly. The average density assigned to each geological unit is related to the main lithology observed in the field according to Telford *et al.* (1990): 2.30g/cm<sup>3</sup> for the Cretaceous marly limestones; 2.65g/cm<sup>3</sup> for the Jurassic carbonates, 2.25g/cm<sup>3</sup> for the Neogene detritic rocks, 2.30g/cm<sup>3</sup> for the evaporites and detritic Triassic rocks, and 2.79g/cm<sup>3</sup> for the basic volcanic rocks.

To solve the structure in the I-I' profile, we considered models with (Fig. 5B) and without (Fig. 5A) hydrogeological continuity between the two carbonate outcrops of Cerro de los Peones and Cabeza Montosa. It was not possible to fit either the gravity anomaly or the

magnetic one with the presence of a diapiric body of Triassic rocks between them that was proposed by Ruiz Reig *et al.* (1988b). The observed relative gravity minimum is up to 4mGal higher than the one calculated in the diapiric model. The best fit was obtained when a synformal geometry of the limestones and the volcanic rocks below the Neogene rocks was considered in the valley between the two hills. The maximum thickness of the main body of volcanic rocks is in the range of 150–200 meters, and it thins concordantly with the Middle–Upper Jurassic limestones along the northern limb of the synform. Its interstratified character points to the hydrogeological continuity hypothesis. The maximum thickness of the Neogene sedimentary rocks cropping out in the valley is 150–200m.

The II-II' gravity model (Fig. 5C), located from Cabeza Montosa towards the western sector of the LSL aquifer, suggests the continuity of the folded Cretaceous and Jurassic limestones below the eastern half of the Neogene-Paleogene outcrops. However, the presence of low permeable Triassic marls between the limestones and the detritic cover at the eastern edge of the profile may isolate both sectors of the LSL aquifer. More geophysical data are necessary to confirm this hypothesis. Towards the west, the model also points to the pinch-out of the carbonate formations.

**Magnetic model**

The most remarkable feature in the magnetic anomaly map (Fig. 4B) is the magnetic dipole whose minimum is located to the north of Cabeza Montosa (-389nT), and maximum (+223nT) to the south of the same hill. Qualitatively, it corresponds to an equidimensional or E–W elongated body placed in between the maximum and

the minimum of the dipole, with a positive contrast on the magnetic susceptibility. It may be related to the presence of basic pillow lavas interstratified between the Jurassic carbonate rocks. A 2D magnetic model (I–I’'), located over this dipole, was performed to discern the shape and depth of the anomalous magnetic body. The minimum and maximum values along the profile are -327nT and +223nT, respectively. For modeling purposes, the reference level of

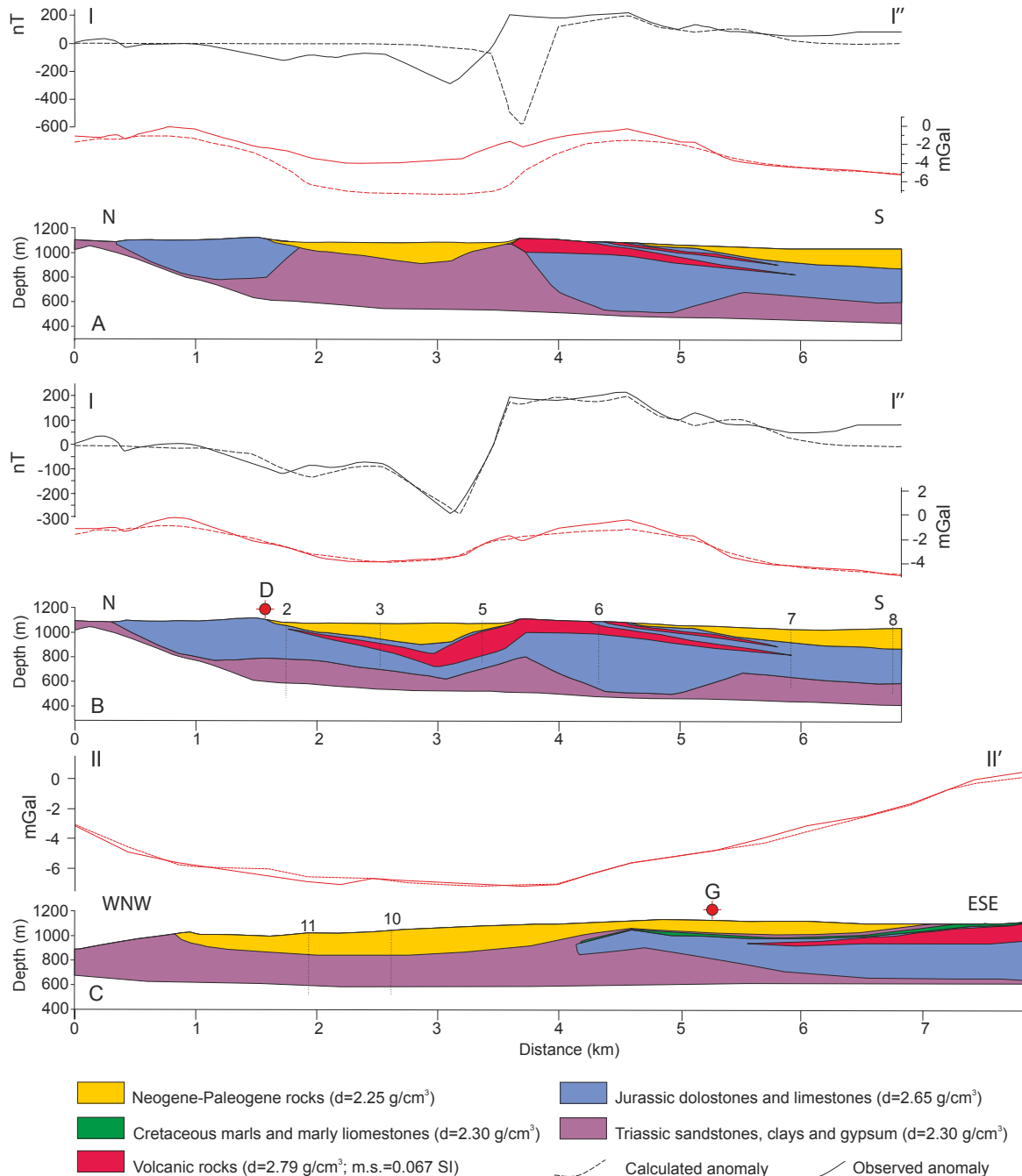


**FIGURE 5.** A–B) 2D integrated gravity and magnetic models of profile I–I'' and C) II–II' gravity model. For the I–I'' profile, models A) without and B) with hydrogeological continuity are shown (d: density; m.s.: magnetic susceptibility). Numbers along the profiles represent TEM soundings; capital letters mark wells position as in Figure 1.

the magnetic anomaly was displaced 40nT to fit the zero value, as a consequence of overestimation of the IGRF 2010 in the study area.

Field measurements of magnetic susceptibility in the pillow lavas give a mean value of 0.016SI, which is in the range proposed for these rocks (Telford *et al.*, 1990). A radial pattern was observed, with increasing magnetic susceptibility towards the core of the pillow lavas. However,

the best fit of the model is obtained considering 0.067SI, higher than field measurements, which implies the existence of remnant magnetization. The higher susceptibility value modeled is justified, as magnetic modelling accounts for the contrast in magnetic susceptibility and parallel remanent magnetism in rocks with high Königsberger ratio values (remanent to induced magnetization). The model without hydrogeological continuity (Fig. 5A) cannot fit the magnetic dipole minimum in its real position.

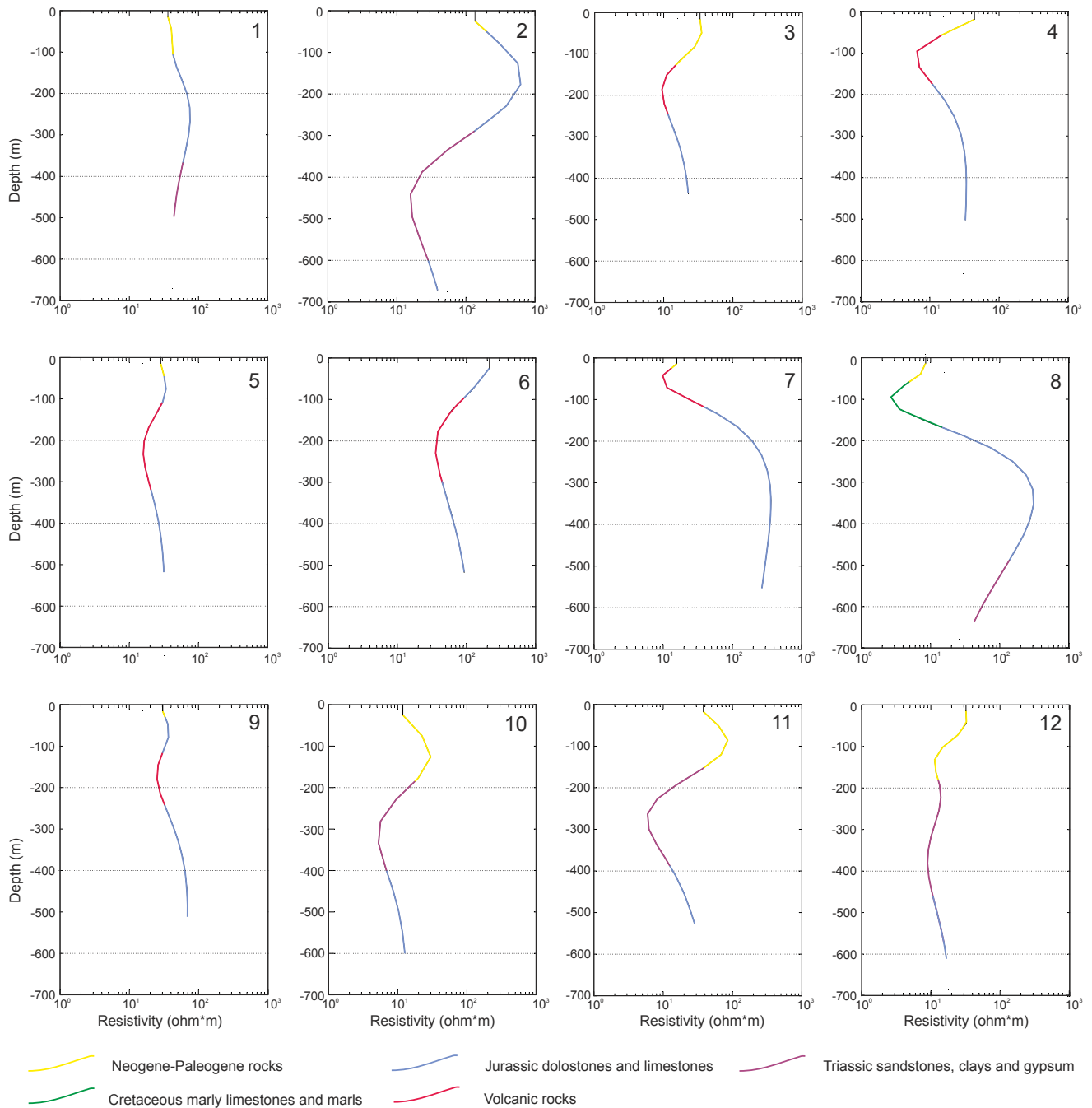


**FIGURE 6.** TDEM resistivity-versus-depth curves (obtained through smooth-model inversion of the apparent resistivity data) and geological interpretation. Colours as in Figure 5.



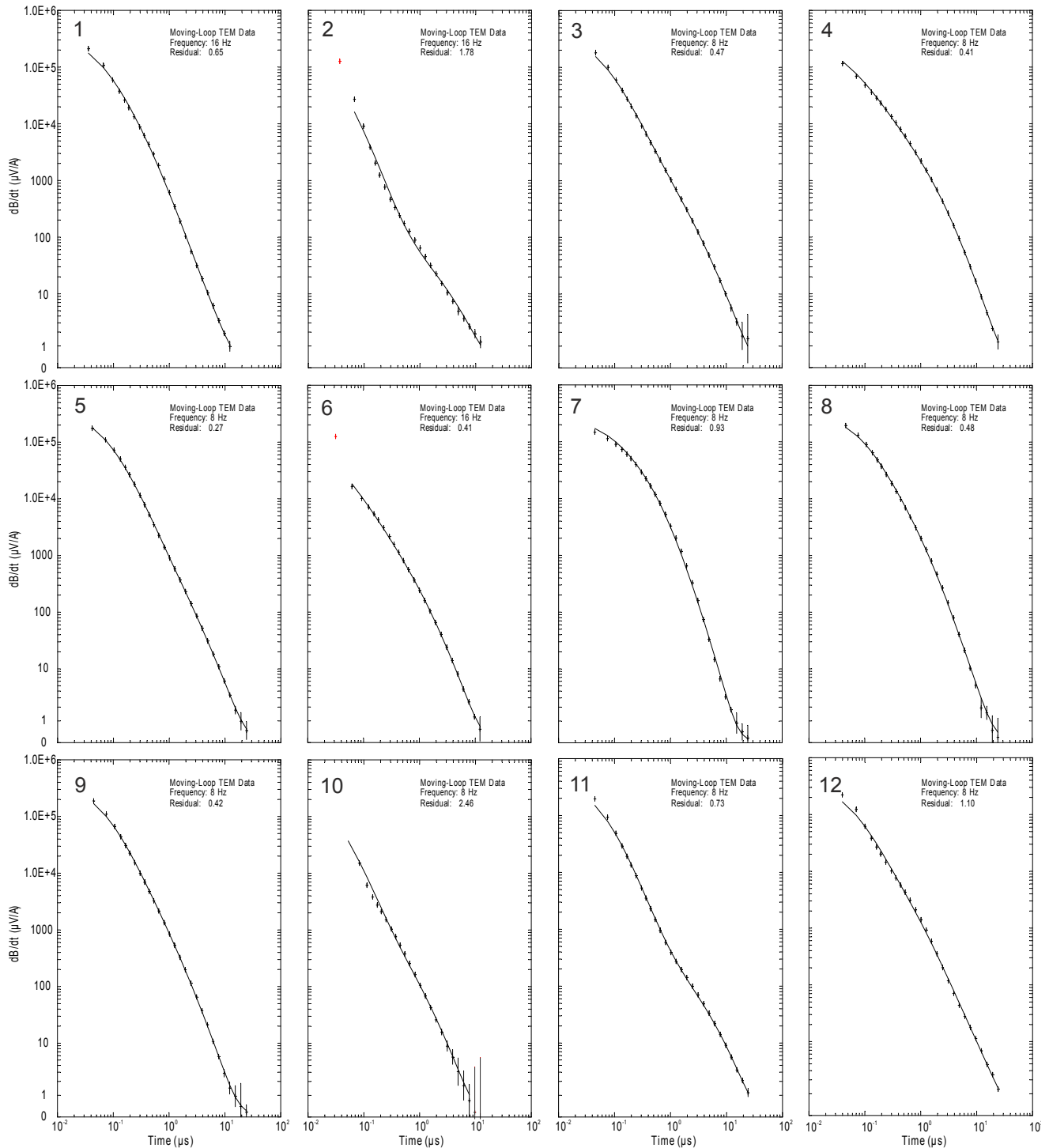


FIGURE 7. 1D inversion of the TDEM data acquired. Crosses represent apparent resistivity vs. time field data and the line shows the best model fitting.

The joint modeling of both gravity and magnetic anomalies therefore enables us to better establish the deep geometry of the volcanic rocks and the limestones, as their continuity in the synform below the valley would justify both anomalies and support the hydrogeological continuity of the LSL and LSG aquifers.

**TDEM soundings**

The 1D apparent resistivity curves do not uniquely resolve the thickness and resistivity of a layer from its conductance value (thickness/resistivity ratio) as different combinations could obtain the same ratio

without appreciable variation in the apparent resistivity curve. However, the distribution of TDEM soundings, focusing on the main transects studied through magnetic and gravity models, provides new constraints and better resolution to derive a reliable geological structure for use in hydrogeological interpretation. Keeping in mind that we obtain apparent resistivity values, we yield information about the alternation of conductive and resistive layers.

Figure 6 shows results from the TDEM soundings and Figure 8 their position in the geological profile. In the profile I (soundings 1-9), volcanic rocks are measured as conductive layers of variable thickness (80–250m) interbedded between resistive bodies of limestones (30–600Ohm·m, depending on the degree of fracturation). The low resistivity values (10–400Ohm·m) of the volcanic rocks may be related to metallic mineralizations produced during the volcanic process and their thickness is conditioned by their position in the folded structure. Below them, conductive rocks related to the presence of Triassic clays (15–500Ohm·m) seal the aquifer, although their bottom is only reached in a sounding (sounding 2, with a thickness of ~200m). The range of apparent resistivity values of the volcanic and the Triassic rocks are very similar. However, knowledge of the geological structure and the stratigraphic succession allow discerning among them.

The amount of information provided by the TDEM data in the II–II' profile (10–12 soundings; Fig. 6) is more limited but points to the presence of Triassic clays and gypsum just below the alternating marls and calcarenites (conductive and resistive layers up to 150–200m depth) that constitute the western detritic aquifer sector. These rocks would seal the aquifer, entailing hydrogeological disconnection. Although this is the most probable structure, borehole data appear to be necessary to confirm the structure of the WNW part of the model (Fig. 5C). The high resistivity values at the bottom of the curves could be related to the presence of alternations of Triassic sandstone levels but also to resistive Jurassic limestones below the Triassic conductive rocks.

### Tectonic structure

The tectonic structure of the LSL aquifer was constrained, with field observations, paying special attention to its limit with the LGC (Fig. 8). Cabeza Montosa is a N100°E antiform vergent to the N with a southern limb dipping 25–50°. In the northern one, bedding is not clearly recognized; interstratified submarine basalts crop out as erosion has removed part of the Upper Jurassic oolitic limestones. Striated bed surfaces with reverse kinematics were observed, suggesting flexural slip during the folding of these units. The western border of Cabeza Montosa is the periclinal end of the antiform. Its structure

is similarly affected by N50°E normal faults, and another set of N–S faults cutting the main ones. To the north, Cerro de los Peones is a monoclinical of Lower Jurassic dolostones with a southern limb dipping 55°. The continuity between these two carbonate outcrops is covered by Neogene rocks, although geophysical data point to their connection through a synform. The Lower Jurassic dolostones of the northern face show diffuse bedding due to dolomitization/dedolomitization processes. They, in turn, are superposed onto Triassic clays, sandstones and gypsum showing ductile deformation structures. To the N of Cerro de los Peones, folded Triassic clays, gypsum and dolostones crop out along a 1km wide valley.

### DISCUSSION

Groundwater is extremely important for the water supply in rural areas as its proximity to demand location diminish the scale of distribution and storage infrastructures reducing the investment requirements (Foster *et al.*, 2006). However, the development and expansion of villages and small-towns underlain by minor aquifers has rarely been planned in terms of water supply management. In such context, the combination of hydrogeological and geophysical investigations provides valuable information of these areas whose access to water wells is limited and not very predictable.

The spatial distribution of the piezometric levels suggests a certain degree of hydrogeological compartmentalization in the LSL aquifer. Springs and wells of the western detritic sector have piezometric levels around 1000m.a.s.l. Data from Molino del Barranco spring (C, 932m.a.s.l.), and the well of Cerro de Los Peones (D, 944m.a.s.l.), in the eastern carbonate sector, suggest there is no hydrogeological connection between the two sectors. The II–II' gravity model (Fig. 5C) points to the absence of Jurassic carbonate rocks in contact with the Paleogene to Plio-Quaternary rocks cropping out in the WNW half of the profile. This would also indicate groundwater disconnection between both sectors but further piezometric data are required to confirm this feature. At the northern border, the presence of low permeable Triassic clays and gypsum at heights greater than 1000m.a.s.l., also implies a barrier to groundwater flow towards the north of the LSL aquifer. However, water circulation through the Triassic sandstones can't be ruled out. Scarce hydrogeological information (absence of piezometric control and hydrographs of the main springs) prevents establishing a hydrogeological conceptual model of the aquifer.

The average recharge rate in the Miocene rocks (Mancera, 2013) is in the range 60–80mm/year, which would imply an annual average rate of 0.45–0.60hm<sup>3</sup>/year for the 7.53km<sup>2</sup>

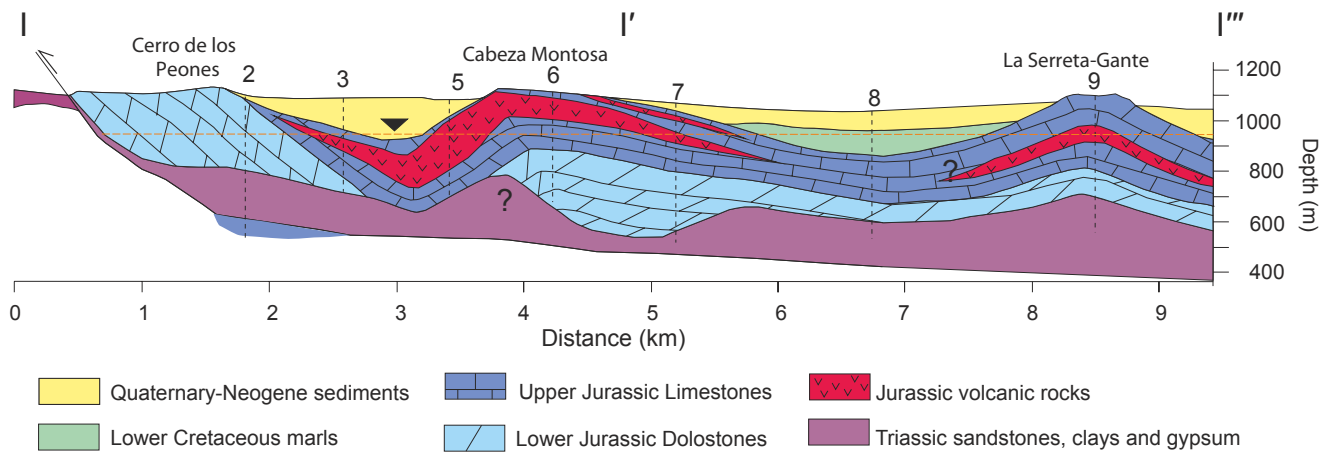


**FIGURE 8.** Interpretative geological cross-section of profile I-I'''. The piezometric level of July 2013 is marked.

of permeable outcrops. Similarly, considering an average saturated thickness of 90m and average porosity values of 8% (Pulido-Bosch *et al.*, 2004), the total groundwater reserves are 54hm<sup>3</sup>. The increasing exploitation of the Miocene aquifer for the irrigation of olive groves and the absence of hydrogeologic control demand sustainable management policies to reduce water consumption in order to avoid water shortage and the lowering of groundwater quality as a consequence of mixing with mineralized groundwater from the Triassic aquitard.

Likewise, piezometric levels at LSL and LGC aquifers (932m.a.s.l. in Molino del Barranco spring, 944m.a.s.l. in Cerro de los Peones well and 939m.a.s.l. in Molino de Gante spring) point to the open character of the SE boundary and the existence of a hydrogeological connection due to the continuity of the permeable carbonate rocks (Fig. 5A and 5B; Profile I-I'''). This information is relevant when determining the storage reserves available for water supply to the nearby villages. The cumulative decrease in dry periods of the piezometric level at Cerro de los Peones (April 2004–August 2009) was 34m. This fact can be explained by the presence of lateral barriers of null flow (*i.e.* the northern boundary) that accelerate the decrease of the pumping cone. In wet periods, in contrast, the recharge of a larger aquifer leads to the faster recovery of the groundwater level in this sector.

The annual average recharge rate at the carbonate outcrops (2.21km<sup>2</sup>) of Cerro de los Peones and Cerro Los Chotos is in the range 0.2–0.3hm<sup>3</sup>/year, with average values for these rocks of 100–120mm/year (Mancera, 2013). During dry periods, groundwater exploitation produces the depletion of springs nearby the Cerro de los Peones well and the decreasing of groundwater quality. Therefore, the low recharge rate and the nearby presence of evaporitic Triassic rocks require a greater groundwater control in both sectors.

Gravity and TDEM studies are widely used in hydrogeological research to constrain the geometry of aquifers (Duque *et al.*, 2008; Bedrosian *et al.*, 2013; Martos-Rosillo *et al.*, 2014). Despite the widespread occurrence of mafic and ultramafic volcanic rocks interlayered within sedimentary beds, magnetic studies of aquifers are less common (Finn and Morgan, 2002; Mishra and Vijay Kumar, 2005). For example, the Miocene detritic formations in the central part of the United States enclose the Ogallala-High Plains Aquifer, one the largest aquifers in the world (Basso *et al.*, 2013). These rocks are broadly interlayered with basalts (*e.g.* Izett, 1975) leading to magnetic anomalies (*e.g.* Zietz and Kirby, 1972). There are many examples worldwide of carbonate aquifers that include basalt parallel to the bedding or at the base of the carbonate sequence. For instance, Triassic tholeiitic basalts, which could be identified using magnetic studies, are frequently located at the base of the carbonate aquifer in the Moroccan Central High Atlas (*e.g.* Teixell *et al.*, 2003). In south China, there are also some examples of limestone interlayered with volcanic rocks where magnetic prospecting could help to constrain the structure of reservoirs (Cheng *et al.*, 2012). The joint modelling of both gravity and magnetic anomalies therefore enables us to better establish the deep geometry of the volcanic and carbonate rocks, as their continuity in the synform below the valley would support the hydrogeological continuity between the LSL and LSG aquifers.

As in other geophysical studies using potential field methods, we emphasize the necessity to use additional information such as other geophysical techniques and/or geological data to better constrain the derived models. This case study may stand as a good example where a magnetic study was crucial to resolve a hydrogeological problem, and where TDEM, gravity and geological information were used to constrain the possible solutions.

## CONCLUSIONS

The integration of gravity and magnetic data with the classical electromagnetic methods provide good results to constrain the deep geometry of small size carbonate aquifers with intercalated volcanic basic rock layers. While magnetic and TDEM data constrain the geometry of the volcanic rocks, gravity data make it possible to test the presence in depth of high permeable limestones instead of low permeable clays and evaporites.

The hydrogeological continuity of LSL and LGC aquifers is suggested by the fast recovery of the piezometric levels in the water-supply wells and the similarity of the heights measured at the springs. In addition, the joint modeling of gravity, magnetic and TDEM data points to the absence of a prominent Triassic diapir disconnecting the carbonate rocks constituting the hills of Cerro de los Peones and Cabeza Montosa. The tectonic structure is formed by a synform of Jurassic permeable carbonates with interstratified volcanic rocks. Such evidence suggests a need to redefine the limits of these formerly disconnected aquifers, and would explain the increase in the volume of the carbonate reservoir. In addition, gravity and TDEM data enabled us to define the depth and geometry of the low permeable Triassic substratum. The contact of the evaporitic Triassic rocks with the permeable Jurassic limestones/Miocene calcarenites, together with the low recharge rate and the reduced storage capability of the Miocene aquifer require a strict control of groundwater exploitation (volume, groundwater quality and evolution of the piezometric level). This information about the connection or disconnection of small size aquifers seems essential to define a groundwater sustainable yield in this region.

## ACKNOWLEDGMENTS

This work was financed by the Diputación Provincial de Jaén and through the project CGL-2010-21048, and the Junta de Andalucía group RNM148 and P09-RNM-5388.

## REFERENCES

- Ayarza, P., Alvarez-Lobato, F., Teixell, A., Arbolea, M.L., Tesón, E., Julivert, M., Charroud, M., 2005. Crustal structure under the central High Atlas Mountains (Morocco) from geological and gravity data. *Tectonophysics*, 400, 67-84.
- Bakalowicz, M., 2005. Karst groundwater: a challenge for a new resources. *Hydrogeology Journal*, 13, 148-160.
- Basso, B., Kendall, A., Hyndman, D.W., 2013. The future of agriculture over the Ogallala Aquifer: Solutions to grow crops more efficiently with limited water. *Earth's Future*, 1, 39-41.
- Bedrosian, P.A., Burgess, M.K., Nishikawa, T., 2013. Faulting and groundwater in a desert environment: constraining hydrogeology using time-domain electromagnetic data. *Near Surface Geophysics*, 11(5), 545-555.
- Chalikakis, K., Plagnes, V., Guerin, R., Valois, R., Bosch, F.P., 2011. Contribution of geophysical methods to karsts-system exploration: an overview. *Hydrogeology Journal*, 19, 1169-1180.
- Chambers, J., Kuras, O., Meldrum, P., Ogilvy, R., Hollands, J., 2006. Electrical resistivity tomography applied to geologic, hydrogeologic, and engineering investigations at a former waste-disposal site. *Geophysics*, 71(6), B231-B239.
- Cheng, Y., Mao, J., Rusk, B., Yang, Z., 2012. Geology and genesis of Kafang Cu-Sn deposit, Gejiu district, SW China. *Ore Geology Reviews*, 48, 180-196.
- Dafflon, B., Irving, J., Holliger, K., 2009. Use of high-resolution geophysical data to characterize heterogeneous aquifers: Influence of data integration method on hydrological predictions. *Water Resources Research*, 45, W09407.
- Duque, C., Calvache, M.L., Pedrera, A., Martín-Rosales, W.M., López-Chicano, M., 2008. Combined time domain electromagnetic soundings and gravimetry to determine marine intrusion in a detrital coastal aquifer (Southern Spain). *Journal of Hydrology*, 349, 536-547.
- Finn, C. A., Morgan, L.A., 2002. High-resolution aeromagnetic mapping of volcanic terrain, Yellowstone National Park. *Journal of Volcanology and Geothermal Research*, 115, 207-231.
- Foster, S., Tuinhof, A., Garduño, H., Kempe, K., Koundouri, P., Nanni, M., 2006. Groundwater Resource Development in Minor Aquifers. Management strategy for village and small town water supply. *GW Mate Briefing Notes*, 13.
- García-Hernández, M., López-Garrido, A.C., Rivas, P., Sanz de Galdeano, C., Vera, J.A., 1980. Mesozoic palaeogeographic evolution of the External Zones of the Betic Cordillera. *Geologie en Mijnbouw*, 59(2), 155-168.
- Gibson, P.J., Lyle, P., George, D.M., 1996. Environmental applications of magnetometry profiling. *Environmental Geology*, 27, 178-183.
- Hammer, S., 1982. Critique of Terrain Corrections for Gravity Stations. *Geophysics*, 47, 839-840.
- IAGA Working Group V-MOD, 2010. International Geomagnetic Reference Field: the eleventh generation. *Geophysical Journal International*, 183(3), 1216-1230.
- IGME-DPJ, 2011. Atlas hidrogeológico de la provincia de Jaén. Eds. Instituto Geológico y Minero de España, 142-151.
- ITGE, 1990. Informe final de la perforación y aforo realizados para abastecimiento en el término municipal de Cabra del Santo Cristo (Jaén). [http://www.igme.es/internet/sistemas\\_infor/ConsultaSID/presentacion.asp?Id=4081](http://www.igme.es/internet/sistemas_infor/ConsultaSID/presentacion.asp?Id=4081)
- Izett, G.A., 1975. Late Cenozoic Sedimentation and Deformation in Northern Colorado and Adjoining Areas. *Geological Society of America Memoir*, 144, 179-210.
- Karner, G.D., Studinger, M., Bell, R.E., 2005. Gravity anomalies of sedimentary basins and their mechanical implications;

- Application to the Ross Sea basins, West Antarctica. *Earth and Planetary Science Letters*, 235, 577-596.
- Kirsch, R., 2009. *Groundwater geophysics a tool for hydrogeology*. Berlin, Springer, 556pp. Website: <http://public.eblib.com/EBLPublic/PublicView.do?ptiID=603393>
- La Femina, P.C., Connor, C.B., Stamatakis, J.A., Farrell, D.A., 2002. Imaging an active normal fault in alluvium by high-resolution magnetic and electromagnetic surveys. *Environmental and Engineering Geoscience*, 8, 193-207.
- Mancera, E., 2013. Evaluación de la recarga en un acuífero carbonático sometido a explotación intensiva. El acuífero de Bedmar-Jodar (Jaén). Master Thesis. Universidad de Málaga, Spain, 78pp.
- Martos-Rosillo, S., Marín-Lechado, C., Pedrera, A., Vadillo, I., Motyka, J., Molina, J.L., Ortiz, P., Martín-Ramírez, J.M., 2014. Methodology to evaluate the renewal period of carbonate aquifers: a key tool for their management in arid and semiarid regions, with the example of Becerrero aquifer, Spain. *Hydrogeology Journal*, 22, 679-689.
- Mishra, D.C., Vijay Kumar, V., 2005. Evidence for Proterozoic collision from airborne magnetic and gravity studies in Southern Granulite Terrain, India, and signatures of recent tectonic activity in the Palghat Gap. *Gondwana Research*, 8(1), 43-54.
- Nielsen, L., Jørgensen, N.O., Gelting, P., 2007. Mapping of the freshwater lens in a coastal aquifer on the Keta Barrier (Ghana) by transient electromagnetic soundings. *Journal of Applied Geophysics*, 62(1), 1-15.
- Pedley, R.C., Busby, J.P., Dabeck, Z.K., 1993. *Gravmag User Manual- Interactive 2.5D gravity and magnetic modelling*. British Geological Survey. Technical Report, WK/93/26/R, 75pp.
- Pedrera, A., Marín-Lechado, C., Galindo-Zaldívar, J., García-Lobón, J.L., 2013. Control of preexisting faults and near-surface diapirs on geometry and kinematics of fold-and-thrust belts (Internal Prebetic, Eastern Betic Cordillera). *Journal of Geodynamics*, 77, 135-148.
- Pérez-López, A., 1991. El Trías de facies germánica del sector central de la Cordillera Bética. PhD Thesis. Universidad de Granada, Spain, 400pp.
- Pérez-López, A., 1996. Sequence model of coastal-plain depositional systems of the Upper Triassic (Betic Cordillera, southern Spain). *Sedimentary Geology*, 101, 99-117.
- Peters, L.J., 1949. The direct approach to magnetic interpretation and its practical application. *Geophysics*, 14, 290-320.
- Pulido-Bosch, A., Motyka, J., Pulido-Leboeuf, P., Borczak, S., 2004. Matrix hydrodynamic properties of carbonate rocks from the Betic Cordillera (Spain). *Hydrological Processes*, 18, 2893-2906.
- Ruiz Reig, P., Álvaro López, M., Hernández Samaniego, A., del Olmo Zamora, P., 1988a. Mapa Geológico Nacional, Escala 1:50.000. Hoja 948 (Torres). Instituto Geológico y Minero de España (IGME).
- Ruiz Reig, P., Díaz de Neira Sánchez, J.A., Enrile Albir, A., López Olmedo, F., 1988b. Mapa Geológico Nacional, Escala 1:50.000. Hoja 970 (Huelma). Instituto Geológico y Minero de España (IGME).
- Ruiz-Constán, A., Galindo-Zaldívar, J., Pedrera, A., Sanz de Galdeano, C., 2009. Gravity anomalies and orthogonal box fold development on heterogeneous basement in the Neogene Ronda Depression (Western Betic Cordillera). *Journal of Geodynamics*, 47(4), 210-217.
- Ruiz-Constán, A., Pedrera, A., Galindo-Zaldívar, J., Pous, J., Arzate, J., Roldán-García, F.J., Marín-Lechado, C., Anahnah, F., 2012. Constraints on the frontal crustal structure of a continental collision from an integrated geophysical research: The central-western Betic Cordillera (SW Spain). *Geochemistry Geophysics Geosystems*, 13(8), 19pp.
- Smyth, H.L., 1896. *Magnetic observations in geological mapping*. American Institute of Mining and Metallurgical Engineers. Transactions, 26, 640-709.
- Soupios, P.M., Kouli, M., Vallianatos, F., Vafidis, A., Stavroulakis, G., 2007. Estimation of aquifer hydraulic parameters from surficial geophysical methods: A case study of Keritis Basin in Chania (Crete-Greece). *Journal of Hydrogeology*, 338, 122-131.
- Teixell, A., Arboleya, M.L., Julivert, M., 2003. Tectonic shortening and topography in the central High Atlas (Morocco). *Tectonics*, 22(5), 1051-1065. DOI:10.1029/2002TC001460.
- Telford, W.M., Geldart, L.P., Sheriff, R.E., 1990. *Applied Geophysics*. Cambridge University press, 792pp.
- Tronicke, J., Holliger, K., 2005. Quantitative integration of hydrogeophysical data: conditional geostatistical simulation for characterizing heterogeneous alluvial aquifers. *Geophysics*, 70(3), H1-H10.
- Vera, J.A., 2004. Cordillera Bética y Baleares. In: Vera, J.A. (ed.). *Geología de España*. Sociedad Geológica de España, Instituto Geológico y Minero de España, 345-464.
- Wantland, D., 1944. Magnetic interpretation. *Geophysics*, 9, 47-58.
- WHYMAP, 2008. *Groundwater Resources of the World*. Map 1:25.000.000. UNESCO, IAH, BGR, CGMW, IAEA. (World-Wide Hydrogeological Mapping and Assessment Programme). Website: [http://www.whymap.org/whymap/EN/Downloads/Global\\_maps/gwrm\\_2008\\_pdf](http://www.whymap.org/whymap/EN/Downloads/Global_maps/gwrm_2008_pdf)
- Zietz, I., Kirby, J.R. Jr., 1972. *Aeromagnetic map of Colorado*. U.S. Geological Survey. Geophysical Series Map GP-880 scale 1:1.000.000.

**Manuscript received November 2014;**  
**revision accepted March 2015;**  
**published Online July 2015.**